RESEARCH ARTICLE
SOLID EARTH: GEODESY AND GRAVITY

Earth and Planetary Physics
6: 241–247, 2022
doi: 10.26464/epp2022025

Theoretical calculation of tidal Love numbers of the Moon with a new spectral element method

BinBin Liao[1], XiaoDong Chen[1,2*], JianQiao Xu[1], JiangCun Zhou[1], and HePing Sun[1,2]

[1]State Key Laboratory of Geodesy and Earth's Dynamics, Innovation Academy for Precision Measurement Science and Technology, Chinese Academy of Sciences, Wuhan 430077, China;

[2]University of the Chinese Academy of Sciences, Beijing 100049, China

Key Points:

- A new spectral element method is proposed for calculating tidal Love numbers of the moon.
- The lunar surface and lunar internal tidal Love numbers are calculated for the 10 main published lunar models.
- The influences of different lunar models on the Love numbers are discussed.

Citation: Liao, B. B., Chen, X. D., Xu, J. Q., Zhou, J. C., and Sun, H. P. (2022). Theoretical calculation of tidal Love numbers of the Moon with a new spectral element method. *Earth Planet. Phys.*, *6*(3), 241–247. http://doi.org/10.26464/epp2022025

Abstract: The tidal Love numbers of the Moon are a set of nondimensional parameters that describe the deformation responses of the Moon to the tidal forces of external celestial bodies. They play an important role in the theoretical calculation of the Moon's tidal deformation and the inversion of its internal structure. In this study, we introduce the basic theory for the theoretical calculation of the tidal Love numbers and propose a new method of solving the tidal Love numbers: the spectral element method. Moreover, we explain the mathematical theory and advantages of this method. On the basis of this new method, using 10 published lunar internal structure reference models, the lunar surface and lunar internal tidal Love numbers were calculated, and the influence of different lunar models on the calculated Love numbers was analyzed. Results of the calculation showed that the difference in the second-degree lunar surface Love numbers among different lunar models was within 8.5%, the influence on the maximum vertical displacement on the lunar surface could reach ±8.5 mm, and the influence on the maximum gravity change could reach ±6 μGal. Regarding the influence on the Love numbers inside the Moon, different lunar models had a greater impact on the Love numbers h_2 and l_2 than on k_2 in the lower lunar mantle and core.

Keywords: lunar tidal Love numbers; spectral element method; solid lunar tides; lunar internal structure reference models; lunar tidal deformation theory

1. Introduction

The solid lunar tides are the periodic deformations that occur on the surface of or inside the Moon under the tidal forces of external celestial bodies such as the Earth and Sun. Because the Moon has no fluid medium such as the ocean or the atmosphere, it has no lunar ocean tide or atmospheric tide; thus, the solid lunar tides can be referred to simply as lunar tides. The theoretical calculation of the lunar tidal deformations follows the basic theory of the traditional solid Earth tidal deformations, and a set of dimensionless Love numbers is usually used to describe the amounts of deformation on the surface of or inside the Moon under the action of the tide-generating potential. The Love number h_n represents the ratio of the radial displacement of a lunar particle to the radial displacement of the static equilibrium tide, the Love number l_n is defined as the ratio of the tangential displacement of a lunar particle to the tangential displacement of the static equilibrium tide, and k_n is defined as the ratio of the additional gravitational potential caused by the tidal deformation to the tide-generating potential, where the subscript n represents the spherical harmonic degree.

During the theoretical calculation process of lunar tidal deformations, the tide-generating potential of external celestial bodies is determined by the mass of the external celestial bodies and their positions relative to the Moon, and these parameters can be calculated very accurately according to the astronomical ephemeris (Simon et al., 1994; Park et al., 2021). Meanwhile, the tidal Love numbers must be obtained by solving the elastic motion equation of the Moon through numerical integration methods.

The significance of the theoretical study of the lunar tidal Love numbers mainly lies in the following two aspects. (1) The values of the lunar tidal Love numbers are closely related to the density distribution, elasticity, and dissipation properties of the internal lunar material and are of great significance for constraining the deep internal layered structure of the Moon (Williams et al., 2014).

Correspondence to: X. D. Chen, chenxd@apm.ac.cn
Received 06 JAN 2022; Accepted 11 MAR 2022.
Accepted article online 28 MAR 2022.

Therefore, the high-precision and high-efficiency forward-modeling algorithm of Love numbers is important for the inversion of the physical property parameters of the deep interior lunar material. (2) At present, only the high-precision observation value of second-degree Love number k_2 can be obtained through space geodetic techniques. Accurate values of other Love numbers cannot be obtained by observations (Garcia et al., 2019); therefore, calculating high-precision tidal Love numbers by using theoretical calculation methods is an important means of obtaining the tidal deformations on the lunar surface. In addition, the lunar tidal deformations calculated by the Love numbers can be an indispensable correction term for future high-precision lunar-based observations.

The key to numerically calculating the lunar tidal Love numbers is solving the elastic motion equations. The governing equations used in the traditional theory of Earth tidal deformation are Poisson's equation and the elastic motion equations derived by Love (1911), in which the Earth's self-gravitation and initial stresses are considered. Alterman et al. (1959) introduced six radius functions y_1–y_6 and transformed the deformation-governing equations into a set of ordinary differential equations about y_1–y_6 by considering the radial inhomogeneity in the layered Earth model. The Runge–Kutta method can then be used to numerically integrate ordinary differential equations so as to obtain the solution to the Earth's deformation problem. However, the traditional Runge–Kutta method has the following two defects. First, it is necessary to obtain three sets of independent solutions before solving the boundary-value problem. However, as the spherical harmonic degree becomes higher, the linear correlation of these three independent solutions increases, which worsens the numerical stability of the deformation solutions (Plag and Jüttner, 1995). Second, in the process of Runge–Kutta numerical integration, the density and elastic modulus are regarded as constants in each step, and the influences of the gradients of these parameters on the results are ignored; thus, errors caused by ignorance are introduced into the results.

To avoid the above-mentioned shortcomings, the Galerkin method, another numerical method of solving partial-differential equations, is adopted in this study. Different from the traditional Runge–Kutta method, the Galerkin method converts the deformation-governing equations in the form of partial-differential equations into weak equations in the form of integral equations and then approximates the weak solutions by using the appropriate basis functions. Consequently, the boundary-value problem can be converted into a linear algebra problem about the coefficients of the basis functions. Studies have shown that the Galerkin method can overcome the shortcomings of the traditional Runge–Kutta method. On one hand, the integral form is used instead of the differential form, thereby eliminating the influence of the density and elastic modulus gradients on the results. On the other hand, in the case of high-degree spherical harmonics, the Galerkin method still has good numerical stability (Quarteroni, 2009). The spectral finite-element method is a Galerkin method proposed by Martinec (2000) that uses spherical harmonic functions and hat functions as basis functions to solve the Earth's loading deformation problem. The authors of the present study have improved on Martinec's spectral finite-element method and proposed a more efficient numerical method, namely, the "spectral element method," which uses higher order polynomial functions instead of hat functions (Liao BB et al., 2019). In this research, the spectral element method is extended to the theoretical calculation of the lunar tidal Love numbers, which is a new numerical algorithm for solving lunar tidal deformations. On the basis of this new algorithm, according to the 10 published internal lunar structure reference models, the respective lunar tidal Love numbers are calculated, and the influence of using different lunar reference models on the calculation of Love numbers is analyzed.

2. Basic Theories of Lunar Tidal Deformations and the Spectral Element Method

Assuming that the Moon is a completely elastic, nonrotating, isotropic, and laterally homogeneous layered sphere, obtaining the lunar tidal Love numbers requires solving the equations governing deformation. The basic theories of lunar tidal deformations and the spectral element method are described in detail below.

2.1 Basic Theory of Lunar Elastic Tidal Deformations

The governing equations of lunar elastic tidal deformations are partial-differential equations composed of the elastic motion equation and Poisson's equation, and they describe the mathematical relationship between the strain tensor and gravitational potential change during the tidal deformation of the Moon. Assuming that the initial stress is hydrostatic pressure, the governing equations of the tidal deformations can be expressed by the following formulas in the frequency domain:

$$\nabla\cdot\boldsymbol{\tau}-\rho_0\nabla\phi_1+\nabla\cdot(\rho_0\boldsymbol{u})\nabla\phi_0-\nabla(\rho_0\boldsymbol{u}\cdot\nabla\phi_0)=\rho_0\omega^2\boldsymbol{u}, \tag{1}$$

$$\nabla^2\phi_1+4\pi G\nabla\cdot(\rho_0\boldsymbol{u})=0, \tag{2}$$

where $\boldsymbol{\tau}$ denotes the stress tensor, $\boldsymbol{u}=(u_r,u_\phi,u_\lambda)$ is the particle's displacement vector, ϕ_1 is the perturbation of the initial gravitational potential ϕ_0, ρ_0 represents the initial density, and ω is the tidal frequency (Dahlen and Tromp, 1998). In addition, for a completely elastic and isotropic material, the constitutive relation between the stress tensor $\boldsymbol{\tau}$ and strain tensor $\boldsymbol{\varepsilon}$ can be expressed as

$$\boldsymbol{\tau}=K\nabla\cdot\boldsymbol{\varepsilon}+2\mu\boldsymbol{\varepsilon}, \tag{3}$$

where K denotes the bulk modulus, μ is the shear modulus, and the relation between the strain tensor and the displacement is

$$\boldsymbol{\varepsilon}=\frac{1}{2}\left(\nabla\boldsymbol{u}+\nabla\boldsymbol{u}^{\mathrm{T}}\right). \tag{4}$$

Equations (1) to (4) are the governing equations of the tidal deformation problem.

The boundary conditions of the equations governing lunar tidal deformation can be expressed by the tide-generating potential of external celestial bodies on the lunar surface, and the specific expressions are as follows:

$$[\hat{\boldsymbol{n}}\cdot\nabla\phi_1+4\pi G\rho_0\hat{\boldsymbol{n}}\cdot\boldsymbol{u}]_-=\hat{\boldsymbol{n}}\cdot\nabla\left(\phi_e+\phi_t^+\right), \tag{5}$$

$$[\hat{\boldsymbol{n}}\cdot\boldsymbol{\tau}]_-^+ = 0, \qquad [\phi_1]_-^+ = 0, \tag{6}$$

where $\hat{\boldsymbol{n}}$ is the unit normal vector of the Moon's outer surface, + and − denote the outer and inner surfaces of the Moon, ϕ_1 is the change in gravitational potential, ϕ_e is the externally applied gravitational force field, and ϕ_t^+ is the tide-generating potential on the Moon's outer surface.

To conveniently compare the relative magnitude between the tide-generating potential ϕ_t^+ and the corresponding lunar surface displacements $\boldsymbol{u}$ and the change in gravitational potential ϕ_1, three dimensionless Love numbers are usually introduced to measure the amounts of tidal deformation. Because the tide-generating potential ϕ_t satisfies the harmonic equation, the tide-generating potential on the Moon's outer surface ϕ_t^+ can be expanded by spherical harmonics. The specific expression is

$$\phi_t^+ = \Sigma_{n=2}^{\infty} W_n = \frac{Gm}{r}\Sigma_{n=2}^{\infty}\left(\frac{R}{r}\right)^n P_n(\cos z), \tag{7}$$

where W_n represents the nth-degree tide-generating potential, r denotes the distance between the centroid of the outer celestial body and the lunar centroid, R is the average radius of the Moon, z is the zenith distance of the outer celestial body relative to the lunar centroid, and P_n represents the nth-degree Legendre polynomial. As with the definition given by Love (1911) and Shida (1912), the relation between Love numbers h_n, l_n, and k_n and the tide-generating potential W_n at each harmonic degree n can be expressed as

$$h_n = \frac{u_r^n}{W_n} g_0, \tag{8}$$

$$l_n = \frac{u_\varphi^n}{\partial W_n/\partial\varphi} g_0, \tag{9}$$

$$k_n = \frac{\phi_e^n}{W_n}, \tag{10}$$

where g_0 represents the initial gravity on the Moon's surface. Tidal Love numbers are very important in the theoretical calculation of tidal deformations. If accurate values of the Love numbers h_n, l_n, and k_n and the tide-generating potential W_n are specified at each spherical harmonic degree, according to Equations (8) to (10), the particle displacement u_r, u_φ and the gravitational potential change ϕ_e can be accurately determined.

Given the boundary-value problem of tidal deformations and the mathematical definition of tidal Love numbers, the problem of obtaining the lunar tidal Love numbers becomes a problem of solving the partial-differential equations. However, because of the inhomogeneity of the internal lunar structure, it is usually impossible to obtain an analytical solution to this problem. Therefore, the only choice is to use numerical methods to solve the aforementioned partial-differential equations.

2.2 Basic Theory of the Spectral Element Method

The spectral element method is a numerical method used to solve second-order partial-differential equations based on their weak solution, and this can transform the boundary-value problem of partial-differential equations into simple algebraic equations (Quarteroni, 2009). Assuming that the solution to the second-order partial-differential equation is the stationary point of a Hermitian bilinear function, then the variation of this Hermitian bilinear function at the stationary point is always equal to zero, and this stationary point is defined as the weak solution of the second-order partial-differential equation. For the tidal deformation-governing Equations (1) to (4), we let Equations (1) and (2) multiply the trial functions $\delta\boldsymbol{u}$ and $\delta\phi$, respectively, and we then integrate them over the Moon. Using Green's theorem, the Lagrangian multiplier method, and the boundary conditions (Equations (5) and (6)), we can obtain the Hermitian bilinear functional

$$K(\boldsymbol{u},\phi;\delta\boldsymbol{u},\delta\phi) = 0, \quad \forall(\delta\boldsymbol{u},\delta\phi)\in W_2^1(V), \tag{11}$$

where the specific expressions of K refer to Martinec's Equations (29) to (33) (Martinec, 2000). In Equation (11), $W_2^1(V)$ represents the Hilbert space, and because it is an infinite-dimensional space, the exact value of the weak solution $(\boldsymbol{u},\phi)$ cannot usually be obtained. To simplify this problem, the Galerkin method is used, and a set of complete basis functions $\{\phi_j\}$ is chosen to form the approximate solution space $W_h(V)$. The spectral element method is a special form of the Galerkin method in which the entire Moon is divided into multiple disjoint elements Ω_k, and a set of orthogonal functions $\{\varphi_{k\alpha}\}$ is selected as basis functions in each element. All these basis functions together constitute the complete basis of the approximate solution space $W_h(V)$ (Quarteroni, 2009).

It should be emphasized here that the spectral element method as used in this research is not the same as that commonly used in seismology. In seismology, the medium is divided into a plurality of tetrahedral or hexahedral elements, and the polynomial functions are used as the basis functions in each element. The advantage is that it can deal with complex models, but the disadvantage is that the computational cost is usually quite large (Komatitsch and Tromp, 1999). However, in this study, considering the lateral homogeneity of the layered lunar model, we divide the entire Moon into several concentric layers Ω_k with different thicknesses. Within each spherical layer, the Lagrange interpolation $f_{k\alpha}(r)$ of a set of Gauss–Lobatto–Legendre control points is selected as the basis function on radius r, and any functions with radius r as a variable can be expanded as follows (Gautschi, 2012):

$$\psi(r) = \sum_k\sum_\alpha \psi^{k\alpha} f_{k\alpha}(r), \tag{12}$$

where k represents the number of concentric spherical layers and α is the number of Gauss–Lobatto–Legendre control points. In addition, for any function with spherical angle $s(\theta,\varphi)$ as variables, the spherical harmonic functions are used as the basis to expand them into a series. Compared with the method used in seismology, the advantage of this method is that it can greatly reduce the computational cost by using the orthogonality of the spherical harmonics. Therefore, the spherical harmonic expansions of the displacement vector $\boldsymbol{u}$ and gravitational potential ϕ_1 can be expressed as follows:

$$\boldsymbol{u}(r,\theta,\varphi) = \sum_{j=0}^{\infty}\sum_{m=-j}^{j}\left[U_{jm}(r)\boldsymbol{S}_{jm}^{(-1)}(\theta,\varphi) + V_{jm}(r)\boldsymbol{S}_{jm}^{(1)}(\theta,\varphi) + W_{jm}(r)\boldsymbol{S}_{jm}^{(0)}(\theta,\varphi)\right], \tag{13}$$

$$\phi_1(r,\theta,\varphi) = \sum_{j=0}^{\infty}\sum_{m=-j}^{j} F_{jm}(r) Y_{jm}(\theta,\varphi), \tag{14}$$

where $Y_{jim}(\theta,\varphi)$ and $\boldsymbol{S}_{jm}^{(\pm1,0)}(\theta,\varphi)$ are scalar and vector spherical harmonics, respectively (Martinec, 2000).

Using the basis function in Equations (12) to (14), we can expand the solution functions $(\boldsymbol{u},\phi)$ and trial functions $(\delta\boldsymbol{u},\delta\phi)$ into a series. Substituting them into the weak solution (11) and letting the coefficients of the trial functions be unit 1, because of the orthogonality of the basis functions, we can obtain the linear algebraic equation about the expansion coefficient vector $\boldsymbol{U}$:

$$\boldsymbol{KU}=\boldsymbol{F}, \tag{15}$$

where $\boldsymbol{K}$ is what is referred to as the "stiffness matrix" and $\boldsymbol{F}$ is an inhomogeneous term. Solving the linear algebraic Equation (15), we can obtain an approximate solution $(\boldsymbol{u},\phi)$ for the boundary-value problem of tidal deformations. Finally, according to the definitions of Equations (8) to (10), the lunar tidal Love numbers h_n, l_n, and k_n can be obtained.

One characteristic of the spectral element method is that it combines the advantages of both the finite-element method and the spectral method and has both high computational efficiency and a high convergence rate. The selection of its basis function is similar to that of the finite-element method. The domain is divided into several disjoint elements so that the stiffness matrix is a sparse matrix with good diagonality, which facilitates solving the linear algebraic equations. In addition, in each element, it is similar to the spectral method and uses a set of orthogonal functions as the basis functions, which can accelerate the convergence of an approximate solution (Quarteroni, 2009).

The spectral element method can be used to calculate the lunar tidal Love numbers accurately, which can be applied to the inverse problem of the interior lunar structure. Because the inversion of the interior lunar structure usually requires forward modeling of a large number of lunar structure models, the computational efficiency of the forward algorithm is one of the key issues in the inverse problem. The spectral element method proposed in this study has high computational efficiency and can be used as an efficient forward algorithm for the inversion of the interior lunar structure.

3. Results of the Lunar Tidal Love Numbers

According to the mathematical theories of the lunar tidal deformation boundary-value problem and the spectral element method given above, the lunar tidal Love numbers are obtained by using the 10 published lunar reference models. The accuracy of the calculated lunar tidal Love numbers depends mainly on the error of the algorithm and the lunar reference model used. The influence of these two aspects on the accuracy of the calculated lunar tidal Love numbers was analyzed.

3.1 Validation of the Spectral Element Method

To validate the new algorithm, it is necessary to compare the lunar tidal Love numbers calculated by the spectral element method with the results calculated independently by other researchers. Using the lunar reference models given by Weber et al. (2011) and Garcia et al. (2011) (denoted "WB11" and "GR11," respectively), Williams et al. (2014) obtained the Moon's second- and third-degree Love numbers h_2, l_2, k_2, h_3, l_3, and k_3. Table 1 compares the calculation results of the spectral element method and the results of Williams et al. (2014). The comparison of results shows that the largest difference appears in the Love number k_3 of the GR11 model, with a relative error of 0.5%. The results in Table 1 verify that the spectral element method can be used for high-precision calculation of the lunar tidal Love numbers.

3.2 Influence of Different Lunar Reference Models on Love Numbers

Owing to the continuous enrichment of lunar observation data and the development of inversion mathematical methods, many lunar reference models have been proposed internationally. The early lunar reference models mainly relied on the constraints of the Apollo moonquake data, in which the density and velocity structure of the lunar mantle could be well constrained by the body wave travel time of moonquakes (Sun et al., 2019). However, because of the low number and poor distribution of Apollo moonquake stations, the travel time of moonquakes cannot well constrain the density and velocity of the lower lunar mantle and core. The early lunar reference models, such as the models of Nakamura (1976) and Gagnepain-Beyneix et al. (2006), do not include the density and velocity structure of the lunar core, so they cannot be used to calculate the lunar tidal Love numbers. Weber et al. (2011) obtained a reference model of the entire moon (i.e., WB11) based on the S-wave travel time inversion, and this model can be used to calculate the lunar tidal Love numbers. With the implementation of lunar exploration programs such as the Gravity Recovery and Interior Laboratory (GRAIL) satellite (Zuber et al., 2013), geodetic observations, such as lunar tide Love number k_2, average density, and average moment of inertia, can be obtained by lunar satellites. These observations can preliminarily constrain the density and velocity structure of the lunar core, but large uncertainties still exist (Matsumoto et al., 2015). Garcia et al. (2011)

Table 1. Love numbers obtained by the spectral element method in this study compared with the results of Williams et al. (2014).

Lunar model		h_2	l_2	k_2	h_3	l_3	k_3
WB11	Williams et al. (2014)	0.0410	0.0107	0.0234	0.0233	0.00300	0.00945
	Present study	0.0410	0.0107	0.0234	0.0233	0.00300	0.00944
Relative error		0.0%	0.0%	0.0%	0.4%	0.0%	0.2%
GR11	Williams et al. (2014)	0.0390	0.0104	0.0223	0.0224	0.00298	0.00910
	Present study	0.0391	0.0104	0.0224	0.0225	0.00298	0.00915
Relative error		0.3%	0.0%	0.4%	0.4%	0.0%	0.5%

combined the P- and S-wave travel times, second-degree Love numbers k_2 and h_2, and other observations to constrain the lunar structure and obtain the lunar reference model GR11. Williams et al. (2014) studied the influence of the thickness of the low-velocity zone and the inner and outer cores on the value of Love number k_2 and provided five lunar reference models, designated GPM1–GPM5. In recent years, Garcia et al. (2019) considered the influence of lunar viscoelasticity on the second-degree Love number k_2 and combined lunar geodetic observation data with moonquake observation data to obtain three lunar reference models, designated M1, M2, and M3. In summary, 10 lunar reference models can presently be used to calculate the lunar tidal Love numbers.

Figure 1 shows the density and Lamé parameters λ and μ of the 10 lunar reference models mentioned at different radiuses. The green lines in Figure 1 are the GPM1–GPM5 models of Williams et al. (2014). The main difference among these five models is the thickness of the inner and outer cores and the low-velocity zone. The pink lines are the three models of Garcia et al. (2019), M1, M2, and M3. Among them, model M3 (dotted line) has the poorest fit, model M1 represents the median values of the posterior probability distribution, and model M2 represents the median values of the 1σ uncertainties. It can easily be seen that the difference among these lunar models is relatively small in the lunar mantle but much larger in the lower lunar mantle and core.

Using the 10 lunar reference models in Figure 1, we calculated the lunar tidal Love numbers, as shown in Table 2. The second- and third-degree Love numbers of the different lunar reference models are given in the table, with the maximum relative error among these models given in the last row. The results in Table 2 show that the maximum relative errors of the second-degree Love numbers h_2, l_2, and k_2 among the different lunar models were 8.5%, 3.8%, and 8.2%, respectively, and those of the third-degree Love numbers h_3, l_3, and k_3 were 4.6%, 5.5%, and 4.2%, respectively. In the following paragraph, we compare these values with the observed values from the GRAIL satellite to illustrate the influence of the different lunar reference models.

Garcia et al. (2019) presented several observation values of the second-degree Love numbers k_2 and h_2, and although the observation value of k_2 is more accurate, that of h_2 has greater uncertainty. The observation value of $k_2 = 0.02294 \pm 0.00018$, which is obtained from the analytical results of the GRAIL satellite's lunar gravity observation data. Table 2 shows that the k_2 of lunar models GPM1–GPM5 is larger than the observation value. This is because Williams et al. (2014) did not consider the effects of viscoelasticity on k_2 when providing lunar models GPM1–GPM5. Regarding Love number h_2, Garcia et al. (2019) pointed out a large disagreement between the h_2 obtained by lunar laser ranging (LLR) and lunar orbit laser altimetry (LOLA), namely that the result for LLR is $h_2 = 0.0450 \pm 0.0058$ and that for LOLA is $h_2 = 0.0353 \pm 0.0031$. In Table 2, the theoretical value of h_2 for different lunar models is in the range of 0.039–0.042, which is within the error range of LLR observations, but it is larger than the value of h_2 given by the LOLA observations.

Because the magnitude of the third-degree tide-generating potential is approximately 0.0045 that of the second-degree tide-generating potential and the magnitude of the higher degree is even smaller than that of the third degree, the calculation error of the theoretical tidal deformations is mainly affected by the second-degree Love numbers. The maximum difference in the

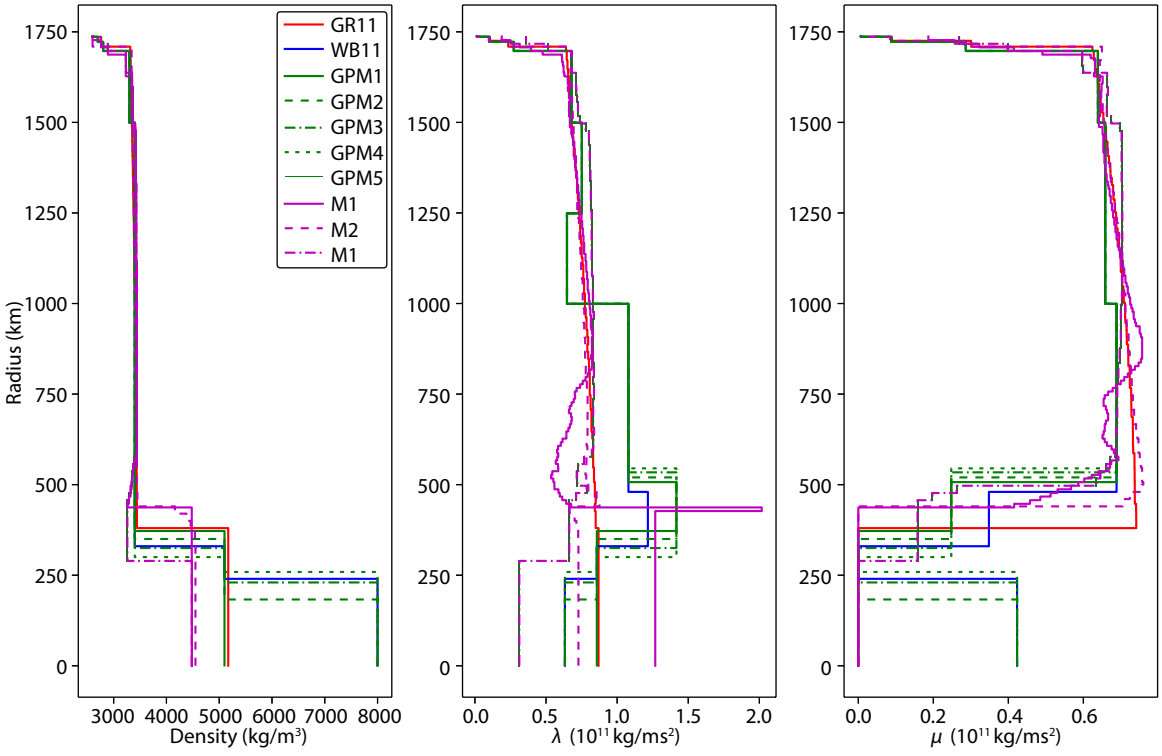

Figure 1. Density and Lamé parameters λ and μ of different lunar reference models at different radiuses.

Table 2. Love numbers of the different lunar reference models calculated by the spectral element method.

Lunar reference model	h_2	l_2	k_2	h_3	l_3	k_3
WB11	0.04095	0.01072	0.02342	0.02326	0.00300	0.00944
GR11	0.03907	0.01044	0.02239	0.02249	0.00298	0.00915
GPM1	0.04235	0.01076	0.02421	0.02343	0.00298	0.00951
GPM2	0.04236	0.01077	0.02421	0.02345	0.00298	0.00951
GPM3	0.04239	0.01077	0.02422	0.02348	0.00298	0.00952
GPM4	0.04240	0.01078	0.02422	0.02351	0.00298	0.00953
GPM5	0.04242	0.01079	0.02423	0.02353	0.00298	0.00954
M1	0.04173	0.01050	0.02383	0.02283	0.00291	0.00924
M2	0.04034	0.01044	0.02308	0.02258	0.00294	0.00920
M3	0.04100	0.01037	0.02360	0.02253	0.00284	0.00923
Maximum	0.00336	0.00041	0.00184	0.00105	0.00016	0.00040
Relative error	8.5%	3.8%	8.2%	4.6%	5.5%	4.2%

second-degree h_2 obtained by the 10 lunar reference models listed in Table 2 is 0.00336, which is less than the observation error of ±0.0058 given by the LLR. Therefore, compared with the observation error, the influence of the different lunar reference models on h_2 can be ignored. Williams et al. (2014) pointed out that the maximum tidal vertical displacement on the lunar surface can reach ±0.1 m. According to Equation (8), the influence of different lunar reference models on the maximum tidal vertical displacement can reach ±8.5 mm, which accounts for approximately 8.5% of the total maximum vertical displacement. Moreover, the change in gravity caused by tidal deformation on the lunar surface is $g = \left(1 + h_2 - \frac{3}{2}k_2\right)\frac{2W_2}{R}$, the maximum value of which can reach approximately ±1 mGal. Therefore, the influence of different lunar reference models on the maximum gravity change can reach ±6 μGal, which accounts for approximately 0.6% of the total. Results showed that the choice of different lunar reference models had a greater impact on the vertical displacement than on the change of gravity.

To study the sensitivity of the lunar tidal Love numbers at different depths to the different lunar reference models, the second-degree Love numbers h_2, l_2, and k_2 corresponding to the 10 lunar reference models were also calculated at different radiuses. Figure 2 shows the radius-profile curves of the second-degree Love numbers of the 10 lunar reference models. The results for

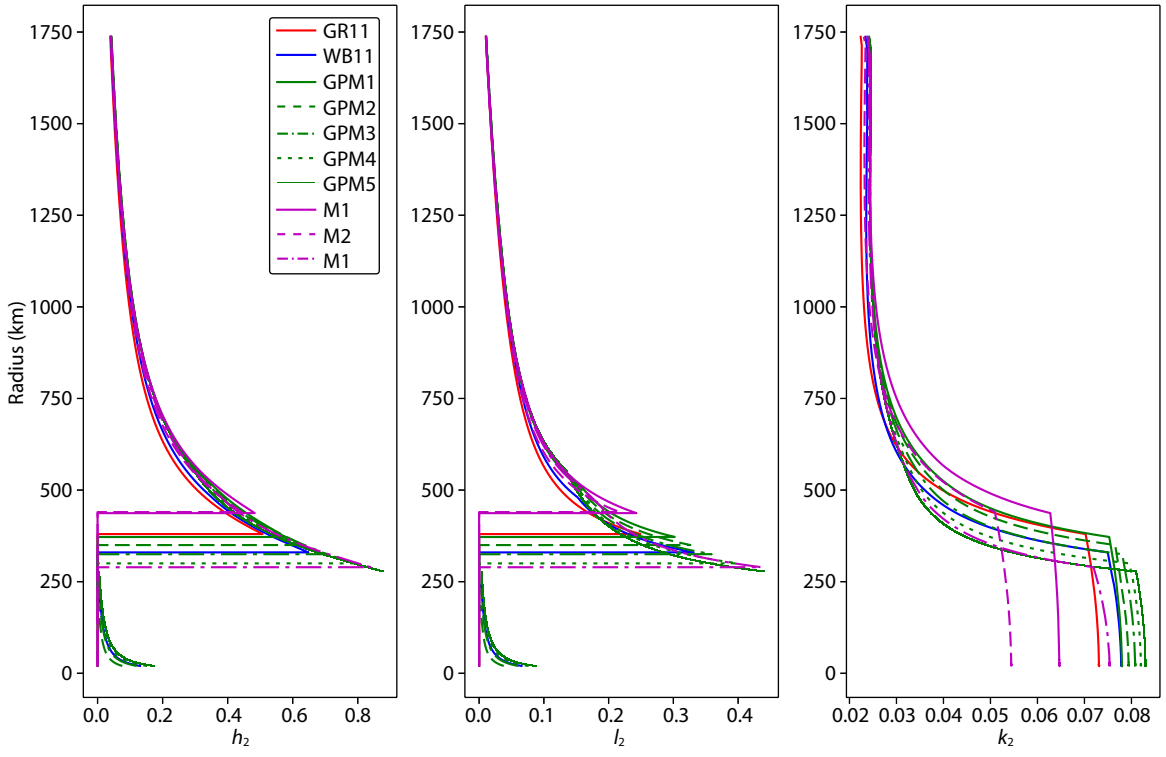

Figure 2. Radius-profile curves of second-degree Love numbers of the 10 lunar reference models.

the lunar surface tide Love numbers showed that they were not sensitive to the deep interior lunar structure. The five green lines in Figure 2 correspond to the lunar reference models GPM1–GPM5 of Williams et al. (2014). Their inner-core radius varies from 0 to 259 km, but the k_2 values vary by only 0.00001. However, for Love numbers h_2 and l_2 in the deep lunar interior, different lunar reference models have an obvious influence on them. At the radius of 500 km, the relative difference of h_2 and l_2 can reach 0.026 and0.012,respectively,amongthe10lunarmodels,whereastherelative difference of k_2 is only 0.008. The numerical results show that, in the deep lunar interior, the Love numbers h_2 and l_2 are more sensitive to the change in lunar reference models than is Love number k_2.

4. Conclusions

The basic theory of the lunar tidal Love numbers is introduced in this study, and a new numerical algorithm, the spectral element method, is proposed to solve for these numbers. The mathematical principles and advantages of the spectral element method are discussed in detail. The tidal Love numbers of the 10 lunar reference models were calculated by using the spectral element method. Using two of the lunar reference models, WB11 and GR11, we compared the second- and third-degree Love numbers calculated by the new method in this study with the calculation results given by Williams et al. (2014). Results showed that the relative error was within 0.5%, which verified that the proposed algorithm is highly accurate.

In addition, we studied the influence of the different lunar reference models on the tidal Love numbers at different depths. The numerical results for the lunar surface tidal Love numbers showed that the relative error of the 10 lunar reference models was within 8.5%, the influence on the maximum vertical displacement on the lunar surface could reach ±8.5 mm, and the influence on the maximum gravity change could reach ±6 μGal. The tidal Love numbers on the lunar surface were not sensitive to parameter changes in the deep interior of the lunar reference models. Regarding the tidal Love numbers in the deep lunar interior, the change in lunar reference models had a greater impact on Love numbers h_2 and l_2 but a small impact on Love number k_2.

Acknowledgments

This study was supported by the Strategic Priority Research Program of the Chinese Academy of Sciences (Grant No. XDB4 1000000), and the National Natural Science Foundation of China (Grant Nos. 42104006, 41974023, 42174101, 41874094, 41874026), and the self-deployed foundation of the State Key Laboratory of Geodesy and Earth's Dynamics (Grant No. S21L6404). We thank LetPub (www.letpub.com) for linguistic assistance during the preparation of this manuscript.

References

Alterman, Z., Jarosch, H., and Pekeris, C. L. (1959). Oscillations of the earth. *Proc. Roy. Soc. Lond. Ser. A, Math. Phys. Sci.*, *252*(1268), 80–95. https://doi.org/10.1098/rspa.1959.0138

Dahlen, F. A., and Tromp, J. (1998). *Theoretical Global Seismology*. Princeton: Princeton University Press.

Gagnepain-Beyneix, J., Lognonné, P., Chenet, H., Lombardi, D., and Spohn, T. (2006). A seismic model of the lunar mantle and constraints on temperature and mineralogy. *Phys. Earth Planet Inter.*, *159*, 140–166. https://doi.org/10.1016/j.pepi.2006.05.009

Gautschi, W. (2012). *Numerical Analysis*. Basel: Birkhauser.

Garcia, R. F., Gagnepain-Beyneix, J., Chevrot, S., and Lognonné, P. (2011). Very preliminary reference moon model. *Phys. Earth Planet Inter.*, *188*, 96–113. https://doi.org/10.1016/j.pepi.2011.06.015

Garcia, R. F., Khan, A., Drilleau, M., Margerin, L., Kawamura, T., Sun, D. Y., Wieczorek, M. A., Rivoldini, A., Nunn, C., … Zhu, P. M. (2019). Lunar seismology: an update on interior structure modes. *Space Sci. Rev.*, *215*(8), 50. https://doi.org/10.1007/s11214-019-0613-y

Komatitsch, D., and Tromp, J. (1999). Introduction to the spectral element method for three-dimensional seismic wave propagation. *Geophys. J. Int.*, *139*(3), 806–822. https://doi.org/10.1046/j.1365-246x.1999.00967.x

Liao, B. B., Xu, J. Q., Sun, H. P., and Zhou, J. C. (2019). Spectral element method to load deformation in a SNREI Earth. *Chin. J. Geophys.* (*in Chinese*), *62*(7), 2382–2393. https://doi.org/10.6038/cjg2019M0043

Love, A. E. H. (1911). *Some Problems of Geodynamics*. Cambridge: Cambridge University Press.

Martinec, Z. (2000). Spectral-finite element approach to three-dimensional viscoelastic relaxation in a spherical earth. *Geophys. J. Int.*, *142*(1), 117–141. https://doi.org/10.1046/j.1365-246x.2000.00138.x

Matsumoto, K., Yamada, R., Kikuchi, F., Kamata, S., Ishihara, Y., Iwata, T., Hanada, H., and Sasaki, S. (2015). Internal structure of the Moon inferred from Apollo seismic data and selenodetic data from GRAIL and LLR. *Geophys. Res. Lett.*, *42*(18), 7351–7358. https://doi.org/10.1002/2015GL065335

Nakamura, Y., Duennebier, F. K., Latheam, G. V., and Dorman, H. J. (1976). Structure of the lunar mantle. *J. Geophys. Res.*, *81*(26), 4818–4824. https://doi.org/10.1029/JB081i026p04818

Park, R. S., Folkner, W. M., Williams, J. G., and Boggs, D. H. (2021). The JPL planetary and lunar ephemerides DE440 and DE441. Astronom. *J.*, *161*(3), 105. https://doi.org/10.3847/1538-3881/abd414

Plag, H. P., and Jüttner, H. U. (1995). Rayleigh–Taylor instabilities of a self-gravitating Earth. *J. Geodynam.*, *20*(3), 267–288. https://doi.org/10.1016/0264-3707(95)00008-W

Quarteroni, A. (2009). *Numerical Models for Differential Problems*. Milan: Springer-Verlag.

Shida, T. (1912). On the body tides of the Earth, a proposal for the international Geodetic Association. *Proc. Tokyo Math.-Phys. Soc. 2nd Series*, *6*(16), 242–258. https://doi.org/10.11429/ptmps1907.6.16_242

Simon, J. L., Bretagnon, P., Chapront, J., Chapront-Touzé, M., Francou G., and Laskar, J. (1994). Numerical expressions for precession formulae and mean elements for the Moon and planets. *Astron. Astrophys.*, *282*(2), 663–683.

Sun, W. J., Zhao, L., Wei, Y., and Fu, L. Y. (2019). Detection of seismic events on Mars: a lunar perspective. *Earth Planet. Phys.*, *3*(4), 290–297. https://doi.org/10.26464/epp2019030

Weber, R. C., Lin, P. Y., Garnero, E. J., Williams, Q., and Lognonné, P. (2011). Seismic detection of the lunar core. *Science*, *331*, 309–312. https://doi.org/10.1126/science.1199375

Williams, J. G., Konopliv, A. S., Boggs, D. H., Park, R. S., Yuan, D. N., Lemoine, F. G., Goossens, S., Mazarico, E., Nimmo, F., … Zuber, M. T. (2014). Lunar interior properties from the GRAIL mission. *J. Geophys. Res.: Planets*, *119*(7), 1546–1578. https://doi.org/10.1002/2013JE004559

Zuber, M. T., Smith, D. E., Lehman, D. H., Hoffman, T. L., Asmar, S. W., and Watkins, M. M. (2013). Gravity Recovery and Interior Laboratory (GRAIL): mapping the lunar interior from crust to core. *Space Sci. Rev.*, *178*(1), 3–24. https://doi.org/10.1007/s11213-012-9952-7